

Determination of the Acidity of Long Chain Alcohols Using Infrared Multiple Photon Dissociation

Jason Wong, David A. Walthall, and John I. Brauman*

Department of Chemistry, Stanford University, Stanford, California 94305-5080

Received: July 8, 2002; In Final Form: September 27, 2002

The acidities of the long chain normal alcohols, 1-pentanol to 1-nonanol, were determined using infrared multiple photon activation of alcohol–alkoxide complexes in an ion cyclotron resonance mass spectrometer. We evaluate the applicability of infrared multiple photon dissociation (IRMPD) as a kinetic method for thermochemical determinations by comparing our results to previous studies using different experimental methods.

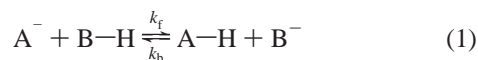
Introduction

In this study we explore the use of infrared multiple photon dissociation (IRMPD) as a “kinetic method” for gas phase thermochemical determinations. In particular, we have used IRMPD to measure the acidities of the long chain alcohols, 1-pentanol to 1-nonanol. Previous investigations of the acidities of these alcohols using kinetic and equilibrium methods have been performed using many different experimental systems.^{1–3} Because we can quantitatively compare our results with other studies, this chemical system can be utilized as a proving ground to assess the viability of our IRMPD method in these types of thermochemical determinations.

The kinetic method, pioneered by Cooks and co-workers, has been utilized for a wide array of thermochemical determinations.^{4–6} The kinetic method has the advantage that it does not depend on pressure measurements. The simplicity of the method permits its implementation on many experimental platforms, including ion cyclotron resonance (ICR), ion kinetic energy (IKE), and mass-analyzed ion kinetic energy (MIKE) mass spectrometers. Given a few important assumptions, the relative product abundances from the dissociation of a common intermediate can give thermochemical information.

In most cases, the kinetic method provides reliable and satisfactory results. More recently, there have been several reports describing the limitations of the general applicability of the kinetic method.^{7–11} These studies address several issues including the validity of the underlying assumptions and the meaning and usage of the effective temperature. Many of these studies have a cautionary tone and point to caveats for applying the kinetic method generally. Several of these authors have developed extensions of the kinetic method both to specifically address inadequacies in the more general form or to extend the utility of the kinetic method in determining additional thermochemical information such as entropy.^{12–14}

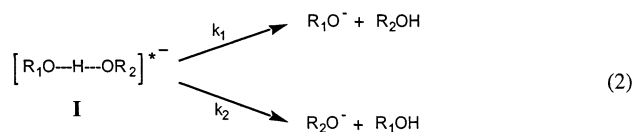
Because the kinetic method does not rely on accurate pressure measurements, it is particularly well suited to the measurement of acidities of low volatility compounds. In other experiments, the relative acidities of AH and BH in eq 1 are determined



directly from the equilibrium constant or from the rates of the

forward and reverse reactions k_f and k_b determined separately ($K = k_f/k_b$). However, in cases where accurate pressure measurements are difficult to obtain, the kinetic method is a convenient alternative. Such is the case with the long chain alcohols, where the vapor pressures of the alcohols are low.

Our experimental method involves the IRMPD of proton bound dimers in an FT-ICR mass spectrometer. The nature of this activation method allows for a high degree of discrimination between competing product branching channels. The product distribution from the dissociation of the energetically activated proton bound dimer (**I**, eq 2) reflects the relative acidities of



the alcohols in the complex. However, because the activation is at low energy, the dissociation products may not quantitatively reflect the acidity difference.

Numerous investigations have reported the acidities of the long chain aliphatic alcohols from 1-pentanol to 1-nonanol with varying results. Higgins and Bartmess determined the acidities to be nonmonotonic with increasing chain length using direct equilibrium methods,¹ whereas other authors have determined a monotonic increase in acidity with chain length using kinetic methods.^{2,3}

In this work, we examine the applicability of our activation scheme for the determination of long chain alcohol acidities. We investigate the influence of several factors, including the energy distribution, effective temperature, and instrumentation differences, to understand the origin of the differences in the results of the various experiments.

Experimental Section

Instrumentation. All experiments were carried out on a Fourier transform ion cyclotron resonance (FT-ICR) mass spectrometer consisting of an electromagnet (0.6 T), vacuum system, and 2.54 cm cubic trapped-ion analyzer cell, interfaced to a FTMS-2000 (IonSpec Corp., Irvine, CA) data acquisition system. The trapped-ion analyzer cell was modified for photochemical experiments by using two IR transparent windows (Melles Griot, 50 mm diameter, 5 mm thick, zinc selenide

coating) and replacing the back plate with a gold-coated copper mirror. All pressures were measured using a vacuum ionization gauge (Varian, model 844). Background pressures were typically 3×10^{-9} Torr and experiments were conducted under operating pressures of 1×10^{-7} to 6×10^{-7} Torr. Data acquisition consisted of at least 200 scans of a standard cycle of 1500 ms (limited by the laser repetition rate) with a 10 ms delay between laser pulse and detection. Each set of data was collected on the same working day; all sets of data were collected within a few working days. Details of the Fourier transform instrumentation can be found elsewhere.¹⁵

Photochemical experiments were conducted with a Lumonics 103-2 CO₂ TEA laser operated multimode with the rear optic as a diffraction grating, allowing line tunable output centered around the 9.6 and 10.6 μm transitions. Details of laser operation have been provided previously.¹⁶ The laser intensity was attenuated using CaF₂ flats of varying thicknesses, and the laser spot size was fixed with a mechanical iris outside the analyzer cell. Laser power was measured using a Scientech Astral AD30 digital laser power meter with a Scientech AC25HDSPL 10.6 μm disk calorimeter.

Materials. Methanol (99.8% purity), methyl formate (97% purity), 1-pentanol (99% purity), 1-hexanol (99% purity), 1-heptanol (98% purity), 1-octanol (99% purity), and 1-nonanol (98% purity), were purchased from Aldrich and were purified by several freeze–pump–thaw cycles before introduction into the machine. 3,3-Dimethyl-2-butanol (98% purity) and 2,2-dimethyl-3-pentanol (97% purity) were purchased from Aldrich and further purified by preparative gas chromatography on a Hewlett-Packard 5790 gas chromatograph equipped with a thermal conductivity detector and a $1/4$ in. diameter, 8 ft. column (Alltech, OV-101 stationary phase on Chromosorb WHP solid support, 80/100 mesh, 10% load). Each gave the appropriate $M - 1$ negative ion peak when reacting with F^- in the FT-ICR. All liquid samples were degassed prior to use with several freeze–pump–thaw cycles.

Dimethyl peroxide was synthesized using a standard laboratory procedure.^{17,18} A 20 mL aliquot of dimethyl sulfate (Aldrich) and 30 mL of 30% hydrogen peroxide solution (Aldrich) were stirred in a 250 mL three-neck flask and cooled to 3 °C with a dry ice/acetone bath. A sample bulb was connected to the three-neck flask through a bubbler and placed in liquid nitrogen to condense the gaseous product. A 40 mL aliquot of 7.5 M KOH solution was added dropwise over 1.5 h through an addition funnel. The entire system was under nitrogen. KOH addition was halted temporarily if the temperature rose above 5 °C. After the addition of KOH was complete, the temperature was allowed to increase to room temperature. The product was degassed on a vacuum line using three freeze–pump–thaw cycles. The product was confirmed by identification of the appropriate parent and $M - 1$ peaks in a positive mass spectrum.

Ion Formation. Primary negative ions were generated by the dissociative electron capture of appropriate neutral precursors at pressures from 1×10^{-7} to 3×10^{-7} Torr. CH_3O^- was generated from CH_3OOCH_3 (eq 3). Methanol–methoxide complex ions were formed by the Riveros reaction^{19,20} at pressures from 3×10^{-7} to 6×10^{-7} Torr (eq 4).



Formation of the desired alcohol–alkoxide complex occurred within 300 ms through neutral alcohol exchange (eqs 5 and 6).

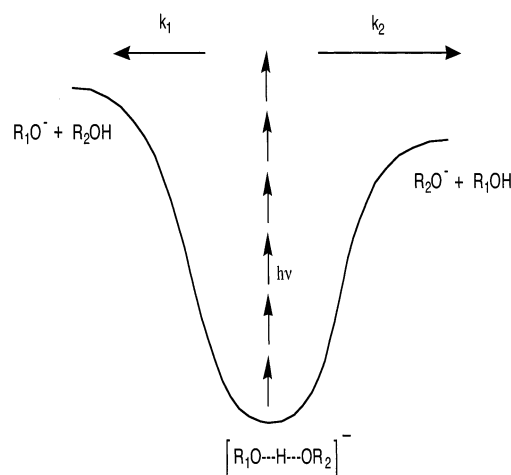
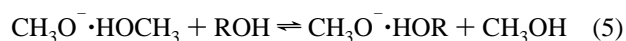


Figure 1. IRMPD of proton bound alcohol-alkoxide complexes.

TABLE 1: Product Ratios $[\text{R}_1\text{O}^-]/[\text{R}_2\text{O}^-]$ from the Dissociation of Proton Bound Dimers of Long Chain Alcohols

R_2O^-	R_1O^-			
	1-nonanol	1-octanol	1-heptanol	1-hexanol
1-pentanol	3.63	2.86	2.36	1.62
1-hexanol	2.83	2.12	1.41	
1-heptanol	2.06	1.70		
1-octanol	1.32			

The desired alcohol–alkoxide complex was isolated by ejecting all other ions from the instrument cell.



Results

A pictorial representation of the infrared multiple photon dissociation (IRMPD) of proton bound dimers is shown in Figure 1. The proton bound dimers are stable alcohol–alkoxide complexes, formed from the association of an alkoxide and an alcohol, as described in the Experimental Section. These complexes are irradiated with infrared photons and decompose to form products when the rate of dissociation to one or both of the product channels (k_1 or k_2 in Figure 1) exceeds the rate of absorption of additional photons. The rate of intramolecular vibrational relaxation (IVR) is extremely rapid ($k \sim 10^{13} \text{ s}^{-1}$)²¹ on the time scale of absorption and dissociation ($k \sim 10^6 \text{ s}^{-1}$).²² Therefore, absorption of photons into any vibrational mode of the molecule is sufficient for activation.

Figure 1 and eq 2 show the dissociation channels of the energetically excited proton bound dimer $[\text{R}_1\text{O} \cdots \text{H} \cdots \text{OR}_2]^-$, where k_1 is the rate constant for the decomposition of the energized complex **I** to give R_1O^- and R_2OH and k_2 is the rate constant for the decomposition of the energized complex **I** to give R_2O^- and R_1OH . Assuming no secondary reactions, the ratio of the rate constants is equal to the ratio of the observed product ions as shown in eq 7.

$$\frac{k_1}{k_2} = \frac{[\text{R}_1\text{O}^-]}{[\text{R}_2\text{O}^-]} \quad (7)$$

IRMPD Results. Table 1 shows the product ratios from all pairs of long chain alcohols. Table 2 lists the ratios of the 1-pentanol, 1-hexanol, and 1-heptanol versus two alcohols with

TABLE 2: Product Ratios of Long Chain Alcohols to Known Alcohols

	1-heptanol	1-hexanol	1-pentanol
3,3-dimethyl-2-butanol	3.85	n/a	0.418
2,2-dimethyl-3-pentanol	<i>a</i>	31.1	n/a

^a This measurement was below the detection limits of our experiment.

TABLE 3: List of Calculated Product Ratios Relative to 1-Pentanol and Calculated Acidities

alcohol	ratio	$\Delta G_{\text{acid}}^{\circ}$ (kcal/mol)
1-pentanol	1.00	367.0
1-hexanol	1.65	366.7
1-heptanol	1.89	366.5
1-octanol	3.12	366.2
1-nonanol	4.01	366.0
2,2-dimethyl-3-pentanol	3.57	364.0
3,3-dimethyl-2-butanol	67.0	366.1

known acidities, 2,2-dimethyl-3-pentanol ($\Delta G_{\text{acid}}^{\circ} = 364.0$ kcal/mol)²³ and 3,3-dimethyl-2-butanol ($\Delta G_{\text{acid}}^{\circ} = 366.1$ kcal/mol).²³ All of the reported ratios are given as the abundance of the larger mass alkoxide divided by the smaller mass alkoxide (i.e., the mass of R_1O^- is larger than that of R_2O^-).

The optimally determined ratios of the 1-alkanols and the known compounds relative to 1-pentanol are listed in Table 3. These ratios were determined from the ratios in Tables 1 and 2 using a least-squares fitting algorithm implemented by a computer program developed in this laboratory, MCSALSA (Monte Carlo Solution for Acidity Ladders by Simulated Annealing).

The photoproduct ratios have been determined from an average of several experiments, done over the course of several working days. Each experiment consisted of an average of at least 200 shots. The shot-to-shot reproducibility of the laser energy was within 5% of the measured power (as measured by the laser power meter). The daily variation in the measurement of these ratios was less than 15%. Because the photoproduct ratios vary less than 10% over a laser energy range of 1.1–2.3 J, an intermediate energy was chosen.

Equilibrium Results. Two semiquantitative equilibrium experiments were performed to measure the relative acidities of 1-pentanol, 1-hexanol, and 1-heptanol. The equilibrium ratios for combinations of pairs of these three compounds were roughly determined in our FT-ICR. Equilibration occurred rapidly (less than 1.5 s), indicating that the forward and reverse reaction rates were near the collision limit and that no volatile impurities were present in the reaction cell. With the pressures of the neutrals approximately the same (as measured by our ion gauge), the relative equilibrium ion concentrations in these three experiments were 1-heptanol > 1-hexanol, 1-hexanol > 1-pentanol, and 1-heptanol > 1-pentanol, suggesting that the order of acidity is 1-heptanol > 1-hexanol > 1-pentanol.

Discussion

Kinetic Method for Long Chain Alcohols. The kinetic method has been utilized in the estimation of a wide range of thermochemical quantities, including proton affinities, ionization energies, and bond dissociation energies.^{4–6} More recently, this method has been applied to structure determination in the quantification of enantiomeric excess in chiral mixtures.²⁴

The foundation for the kinetic method is a correlation between the logarithm of the product branching ratio and the energy difference between the barriers of two competing product channels from a common intermediate.²⁵ In this study, the ratio of the products observed from the unimolecular dissociation of

an alcohol–alkoxide complex reflects the acidity difference between the corresponding alcohols in the complex as shown in eq 8.

$$\ln\left(\frac{[R_1O^-]}{[R_2O^-]}\right) \approx -\frac{1}{RT_{\text{eff}}}(\Delta G_{\text{add}}^{\circ}(R_1OH) - \Delta G_{\text{add}}^{\circ}(R_2OH)) \quad (8)$$

This relationship is not exact and its applicability depends on several factors including the internal energy distribution, the validity of the underlying assumptions, as well as experimental parameters.^{5,8,9,26} Because the two dissociation channels (eq 2) are so similar, we assume that entropy differences are negligible, and in this respect, the kinetic method is especially suitable for the study of these alcohol acidities.

The log-linear relationship has been shown to be valid for branching in highly activated systems with nonthermal energy distributions.^{27–30} The significance of the effective temperature (T_{eff}) has been extensively discussed by several authors.^{7,9,26,31,32} These authors address the validity and usage of T_{eff} and have shown it to be related to characteristics of the dissociating ion population such as size, lifetime, experimental conditions, and internal energy distribution. Using statistical RRK theory, Ervin has derived an analytical expression for T_{eff} applicable for metastable ion decompositions with high ion source temperatures, showing that T_{eff} is directly proportional to the well depth and inversely proportional to the size of the dissociating complex.³¹

Infrared Multiple Photon Dissociation. IRMPD has been widely utilized as an activation method for the study of unimolecular decomposition reactions in several types of investigations.^{16,21,33–35} Other applications have included probing the mechanism of dissociation of tertiary alkoxide ions,^{22,36} determining the acidities of weakly acidic compounds,³⁷ and sequencing large, multiply charged biomolecules.^{38,39} Alcohol–alkoxide complexes have been studied using IRMPD in a variety of investigations.^{40–42}

IRMPD is a low-energy activation method; dissociation to products occurs with a small amount of excess internal energy. This can be reasoned from the relative rates of photon absorption, dissociation (both have $k \sim 10^6$ s⁻¹),²² and IVR ($k \sim 10^{13}$ s⁻¹)²¹ at threshold. Sequential photons are absorbed and the energy is rapidly redistributed in the molecule until the threshold is reached. Just above the threshold, the rates of absorption and dissociation compete so that only one or two more photons can be absorbed before dissociation occurs. This competition in rates corresponds to an excess internal energy of roughly 3–6 kcal/mol.

This low-energy activation has been demonstrated in a previous study in which separate energy dependences in the primary and secondary isotope effects in the IRMPD of selectively deuterated tertiary alkoxide anions were observed.^{22,37} These low-energy activation experiments were performed using both a high-intensity, pulsed infrared source (similar to the method used here) and a low-intensity, continuous-wave infrared source to elucidate the mechanism. Although the energy difference between the dissociation channels was small, attributable to only zero point energy differences, it was possible to observe a difference in rates between these channels. The nature of the activation method allowed a large degree of discrimination between reaction barriers that are relatively close in energy.

The comparison between the low-intensity, continuous-wave and the high-intensity, pulsed infrared sources also gives information about the ion population. Because the continuous-

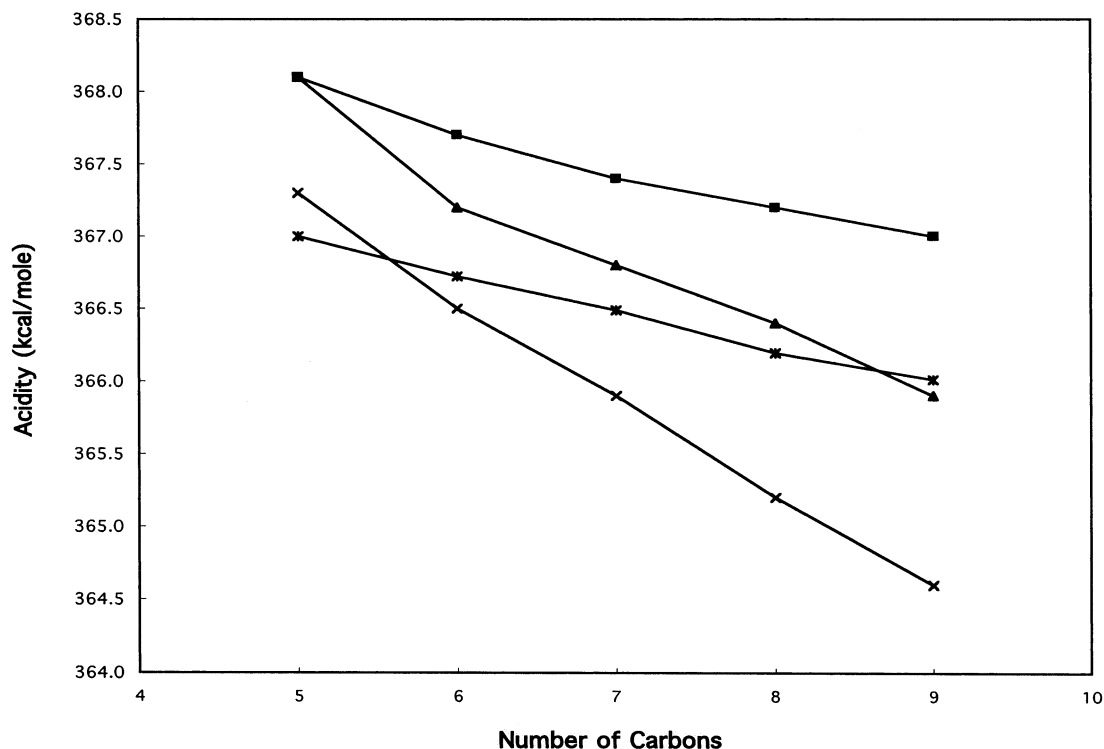


Figure 2. Plot of $\Delta G_{\text{acid}}^{\circ}$ from different experiments using the kinetic method. (×) MIKES; (▲) metastable dissociation; (■) CID; (*) IRMPD.

wave pumping rate is about 5 orders of magnitude slower than the pulsed pumping rate, the species usually dissociate just above threshold for the continuous wave experiments. Therefore, the fraction of ions that dissociate just above threshold for the pulsed infrared source must be very small to give such large differences between the two methods. This shows that our ion populations do not have a significant low energy tail above threshold.

Our method is not suitable for the study of systems in which the relative energy between product channel barriers is large. In these cases, the rate of dissociation through the lower energy channel is much greater than the higher energy channel. Depending on the magnitude of the energy difference, products from the higher energy channel may not be observable.

Another consideration regarding our activation method involves the variation in the energy at which dissociation occurs for different sized complexes. As mentioned above, dissociation occurs when the rate of dissociation is comparable to the rate of photon absorption. The rate of photon absorption will remain fairly constant for different sized complexes because the vibrational frequencies and absorption cross sections do not vary significantly.

Larger complexes have larger density of states at a given energy. Because the microcanonical dissociation rate constant is inversely proportional to the density of states of the complex, the dissociation rate constant will be smaller at a given energy above the threshold in larger systems. Thus, the larger systems must be at relatively higher energy for dissociation to compete with further photon absorption. This increased energy could affect the experimentally observed product branching ratios, making a simple interpretation of an "acidity ladder" difficult.

Table 3 lists the acidity values calculated from the experimental product ratios using eq 8 ($T_{\text{eff}} = 360$ K) and the literature values of the known alcohols. It is evident that our method provides experimental results that are qualitatively similar to other kinetic methods for the measurement of these acidities (i.e., monotonic increase in acidity with chain length).

TABLE 4: Acidities of Alcohols from Previous Studies, $\Delta G_{\text{acid}}^{\circ}$ in kcal/mol

	equil ^a	MIKES ^b	met diss ^c	CID ^c	IRMPD
1-pentanol	367.5	367.3	368.1	368.1	367.0
1-hexanol	367.4	366.5	367.2	367.7	366.7
1-heptanol	368.0	365.9	366.8	367.4	366.5
1-octanol	367.7	365.2	366.4	367.2	366.2
1-nonanol	368.0	364.6	365.9	367.0	366.0

^a Reference 1. ^b Reference 2. ^c Reference 3.

Other Long Chain Alcohol Studies. Table 4 lists acidity values from previous studies as well as our calculated values. Haas and Harrison used a reversed geometry sector (ZAB-2FQ) mass spectrometer to measure acidities using the kinetic method for both metastable dissociation and collision-induced dissociation (at 50 eV) experiments.³ Gäumann and co-workers used the kinetic method on MIKES spectra collected on a reverse geometry sector (ZAB-2F) mass spectrometer.² In contrast to these studies, Higgins and Bartmess measured equilibrium acidity values in an ICR mass spectrometer.¹ To take into account the change in the acidity scale^{23,43} that occurred after the first two studies, Higgins and Bartmess recalibrated the correlation line for the previous two experiments using their experimental ratios and redetermined the absolute acidities. These are the values listed in Table 4.

All of the kinetic method experiments gave alcohol acidities that increased monotonically with increasing chain length. The equilibrium studies by Higgins and Bartmess, however, showed a nonmonotonic correlation of acidity with chain length. Their results were rationalized by examining the overall effect of stabilizing and destabilizing intramolecular interactions in the equilibrium structures of the anions. It was argued that a through-space, chain-wrapping, polarization effect stabilizes the anions whereas gauche interactions and entropy loss associated with the optimal configuration destabilizes the anions.^{1,44} Because the kinetic method can only probe the dissociation characteristics in the transition state, it was implied that the

kinetic method was not applicable for the estimation of the "true" equilibrium acidities.

To confirm this result, we have performed semiquantitative equilibrium studies in our instrument to measure the relative acidities of 1-pentanol, 1-hexanol, and 1-heptanol. With neutral pressures approximately equal, equilibration occurred rapidly, indicating that the forward and reverse reaction rates were near the encounter limit. In contrast to the Higgins and Bartmess work, our studies suggest that the order of equilibrium acidities is 1-heptanol > 1-hexanol > 1-pentanol.

Possible Sources of Differences Among Kinetic Studies. Much of the variation among the kinetic methods can be attributed to differences in experimental apparatus, and as a result, to a variation in the characteristics of the internal energies of the dissociating ion population. The range of values for the entire alcohol series as shown in Table 4 is relatively small for all of the experiments. The largest range of values is 2.7 kcal/mol; our values have a range of 1.0 kcal/mol. Overall, there is not a large variation in acidity values among of the kinetic studies.

Figure 2 shows a plot of all of the absolute acidities determined for each kinetic experiment. The trend lines are all linear but shifted in acidity value relative to one another. We presume that the major source of this discrepancy lies in the method of calibration and the experimental error associated with the calibration. Although several of the calibration compounds overlapped among the experiments, errors associated with the experimentally determined ratios as well as with the least-squares determination would likely produce different absolute acidities.

Relative Acidities. In addition to the shift in the trend lines, each kinetic experiment in Figure 2 exhibits a different slope, indicating a difference in the change in acidity values for each individual experiment (i.e., a variation in $\Delta\Delta G_{\text{acid}}^{\circ}$). The origins of these differences are influenced by several factors, including the internal energy distribution, effective temperature, and experimental apparatus.

It is interesting that the slopes of the lines of our results and the CID results are very similar, whereas the slopes of the metastable dissociation and the MIKES experiment are similar. In the CID experiments and our experiments, all product ions from the dissociation of the complex are collected. The calculated product ratios are therefore integrated over the entire energy range of the dissociating ion population.

This method of collection contrasts with the collection and subsequent detection in the metastable and MIKES experiments, where only fragments from dissociated metastable peaks with a small range of lifetimes are collected. Because the lifetime of a dissociating complex is related to its size and its internal energy, an experimental system comparing different sized complexes is also comparing fragments with different internal energies. This variation in the internal energy of the dissociating ion population is related to T_{eff} varying with the size and the internal energy of the system. An analytical expression explicitly relating T_{eff} to size has been recently shown by Ervin.³¹

The variation in slope also suggests that entropic factors may be playing a modest role (i.e., $\Delta\Delta S_{\text{acid}}^{\circ}$ is not constant). Methods developed by Fenselau and co-workers¹⁴ and Wesdemiotis and co-workers¹³ in which the kinetic method has been extended to determine entropy contributions could conceivably be utilized to estimate these thermochemical values.

Conclusion

We have shown that IRMPD gives satisfactory results as a quantitative method for the determination of acidities using the

kinetic method. Comparing our results to previous results of other kinetic studies shows that discrepancies can be attributed to experimental methods, especially calibration, and that these discrepancies preclude a precise evaluation of the various absolute acidity values. Qualitative comparisons reveal that differences in experimental apparatus and methods are responsible for many of the differences. The effect of the size, internal energy, and lifetime as related to each experiment is critical in utilizing the kinetic method to estimate thermochemical quantities.

In all of the experiments, the dissociating ion population cannot be represented by a Boltzmann distribution but is instead characterized by the effective temperature. Caution must be used when utilizing the effective temperature parameter to compare results between experiments because the distribution of the ion population is not really known.

Acknowledgment. We are grateful to the National Science Foundation for support of this research.

References and Notes

- (1) Higgins, P. R.; Bartmess, J. E. *Int. J. Mass. Spectrom. Ion Processes* **1998**, *175*, 71–79.
- (2) Boand, G.; Houriet, R.; Gäumann, T. *J. Am. Chem. Soc.* **1983**, *105*, 2203–2206.
- (3) Haas, M. J.; Harrison, A. G. *Int. J. Mass. Spectrom. Ion Processes* **1993**, *124*, 115–124.
- (4) Cooks, R. G.; Patrick, J. S.; Kotiaho, T.; McLuckey, S. A. *Mass Spectrom. Rev.* **1994**, *13*, 287–339.
- (5) Cooks, R. G.; Wong, P. S. H. *Acc. Chem. Res.* **1998**, *31*, 379–386.
- (6) McLuckey, S. A.; Cameron, D.; Cooks, R. G. *J. Am. Chem. Soc.* **1981**, *103*, 1313–1317.
- (7) Drahos, L.; Vékey, K. *J. Mass. Spectrom.* **1998**, *34*, 79–84.
- (8) Armentrout, P. B. *J. Mass. Spectrom.* **1998**, *34*, 74–78.
- (9) Cooks, R. G.; Koskinen, J. T.; Thomas, P. D. *J. Mass. Spectrom.* **1999**, *34*, 85–92.
- (10) Holmes, J. L.; Aubry, C.; Mayer, P. M. *J. Phys. Chem. A* **1999**, *103*, 705–709. Erratum. *J. Phys. Chem. A* **1999**, *103*, 6492.
- (11) Thomas, P. D.; Cooks, R. G.; Vékey, K.; Drahos, L.; Wesdemiotis, C. *J. Phys. Chem. A* **2000**, *104*, 1359–1361.
- (12) Armentrout, P. B. *J. Am. Soc. Mass Spectrom.* **2000**, *11*, 371–379.
- (13) Cerda, B. A.; Wesdemiotis, C. *J. Am. Chem. Soc.* **1996**, *118*, 11884–11892.
- (14) Cheng, X.; Wu, Z.; Fenselau, C. *J. Am. Chem. Soc.* **1993**, *115*, 4844–4848.
- (15) Frieser, B. S. In *Techniques in Chemistry Volume 20: Techniques for the Study of Ion-Molecule Reactions*; Farrar, J. M., Saunders, W. H. J., Eds.; John Wiley and Sons: New York, 1988; pp 61–118.
- (16) Johnson, C. E.; Brauman, J. I. In *Techniques in Chemistry Volume 20: Techniques for the Study of Ion-Molecule Reactions*; Farrar, J. M., Saunders, W. H., Jr., Eds.; John Wiley and Sons: New York, 1988; pp 563–589.
- (17) The preparation is adapted from the synthesis reported in: Hanst, P. L.; Calvert, J. G. *J. Phys. Chem.* **1959**, *63*, 104.
- (18) Dodd, J. Ph.D. Dissertation, Stanford University, 1985.
- (19) Faigle, J. F.; Isolani, P. C.; Riveros, J. M. *J. Am. Chem. Soc.* **1976**, *98*, 2049.
- (20) Blair, L. K.; Isolani, P. C.; Riveros, J. M. *J. Am. Chem. Soc.* **1973**, *95*, 1057–1060.
- (21) Lupo, D. W.; Quack, M. *Chem. Rev.* **1987**, *87*, 181–216.
- (22) Tumas, W.; Foster, R. F.; Pellerite, M. J.; Brauman, J. I. *J. Am. Chem. Soc.* **1987**, *109*, 961–970.
- (23) Chase, M. W., Jr. In *J. Phys. Chem. Ref. Data* **1998**, Monograph 9, 1–1951.
- (24) Tao, W. A.; Gozzo, F. C.; Cooks, R. G. *Anal. Chem.* **2001**, *73*, 1692–1698.
- (25) Typically, this log-linear relationship is applied to the study of the unimolecular fragmentation of loosely bound cluster ions but has also been invoked in other systems, such as the dissociation of chemically activated hypervalent silicate compounds (DePuy, C. H.; Bierbaum, V. M.; Damrauer, R. *J. Am. Chem. Soc.* **1984**, *106*, 4051–4053. DePuy, C. H.; Gronert, S.; Barlow, S. E.; Bierbaum, V. M.; Damrauer, R. *J. Am. Chem.*

Soc. **1989**, *111*, 1968–1973) or metal complexes in biological compounds (refs 4, 5, 13, and 14).

(26) Vékey, K. *J. Mass. Spectrom.* **1996**, *31*, 445–463.

(27) Craig, S. L.; Zhong, M.; Choo, B.; Brauman, J. I. *J. Phys. Chem. A* **1997**, *101*, 19–24.

(28) Klots, C. E. *J. Phys. Chem. A* **1997**, *101*, 5378.

(29) Craig, S. L.; Zhong, M.; Choo, B.; Brauman, J. I. *J. Phys. Chem. A* **1997**, *101*, 5379.

(30) Klots, C. E. *J. Phys. Chem.* **1995**, *99*, 1748–1753.

(31) Ervin, K. M. *Int. J. Mass Spectrom.* **2000**, *195/196*, 271–284.

(32) Bojesen, G.; Breindahl, T. *J. Chem. Soc., Perkin Trans. 2* **1994**, *5*, 1029–1037.

(33) Dunbar, R. C. In *Gas-Phase Ion Chemistry*; Bowers, M. T., Ed.; Academic Press Inc.: Orlando, 1984; Vol. 3, pp 129–166.

(34) Farrar, J. M.; Saunders, W. H. *Techniques in Chemistry Volume 20: Techniques for the Study of Ion–Molecule Reactions*; John Wiley and Sons: New York, 1988.

(35) Thorne, L. R.; Beauchamp, J. L. In *Gas-Phase Ion Chemistry*; Bowers, M. T., Ed.; Academic Press: Orlando, 1984; Vol. 3, pp 41–97.

(36) Tumas, W.; Foster, R. F.; Brauman, J. I. *J. Am. Chem. Soc.* **1988**, *110*, 2714–2722.

(37) Wong, J.; Sannes, K. A.; Johnson, C. E.; Brauman, J. I. *J. Am. Chem. Soc.* **2000**, *122*, 10878–10885.

(38) Little, D. P.; Speir, J. P.; Senko, M. W.; O'Connor, P. B.; McLafferty, F. W. *Anal. Chem.* **1994**, *66*, 2809–2815.

(39) Riveros, J. M.; Sena, M.; Guedes, G. H.; Xavier, L. A.; Slepety, R. *Pure Appl. Chem.* **1998**, *70*, 1969–1976.

(40) In a previous article, Baer and Brauman showed that the product distribution from the dissociation of alcohol-alkoxide complexes depended on the method of synthesis. The authors synthesized the same alcohol-alkoxide complex in two ways using the Riveros reaction (Faigle, J. F.; Isolani, P. C.; Riveros, J. M. *J. Am. Chem. Soc.* **1976**, *98*, 2049. Blair, L. K.; Isolani, P. C.; Riveros, J. M. *J. Am. Chem. Soc.* **1973**, *95*, 1057–1060) and observed that the fragments dissociated in a manner that suggested the complexes retained a “memory” of their origin. The magnitude of this differentiation effect, however, was small, and does not affect the results of this study. Baer, S.; Brauman, J. I. *J. Am. Chem. Soc.* **1992**, *114*, 5733–5741.

(41) Tonner, D. S.; McMahon, T. B. *Anal. Chem.* **1997**, *69*, 4735–4740.

(42) Peiris, D. M.; Riveros, J. M.; Eyler, J. R. *Int. J. Mass. Spectrom. Ion Processes* **1996**, *159*, 169–183.

(43) Bartmess, J. E.; McIver, R. T. In *Gas-Phase Ion Chemistry*; Bowers, M. T., Ed.; Academic Press: New York, 1979; Vol. 2, pp 87–121.

(44) Catalán, J. *Chem. Phys. Lett.* **1994**, *221*, 68–70.